24th INTERNATIONAL CONGRESS ON SOUND AND VIBRATION
23–27 July 2017, London

PREDICTION FOR NOISE REDUCTION AND CHARACTERISTICS OF FLOW-INDUCED NOISE ON AXIAL COOLING FAN

Gaku Minorikawa

Hosei University, Department of Mechanical Engineering, Faculty of Science and Engineering, Tokyo, Japan
email: minori@hosei.ac.jp

Tae-Gyun Lim

Technical Research Lab., CEDIC Co. Ltd., Seoul, Korea

Wan-Ho Jeon

Technical Research Lab., CEDIC Co. Ltd., Seoul, Korea

A performance of cooling fan installed at an electronic product should be increased in spite of the decrease of its size. In this study, the noise of a cooling fan was measured in semi-anechoic room, and then compared with the results from computational aeroacoustics (CAA). Three-dimensional Navier-Stokes equations were solved to simulate the unsteady flow field. The simplified Ffowcs Williams and Hawkings (FW-H) equation was used to calculate the noise. The result obtained from CAA agreed with one of the experimental data. The results obtained from CAA results and unsteady flow field showed the sound sources and the noise generation mechanism. One of the dominant sources was the shape of shroud. To reduce the noise, the curvature at the front of the shroud was changed and the reduction of the Overall Sound Pressure Level (SPL) was found in the prediction.
Keywords: aeroacoustics, noise, computational aeroacoustics

1. Introduction

Most of electrical devises have used a cooling module to reduce the internal temperature of them. As the size of products has gotten smaller, the fan size has gotten smaller simultaneously. But to keep remaining the performance of the fan, the rotation speed has increased. With the increase of getting smaller electrical devises, it is difficult to develop the fan with good performance in both the aerodynamics and the aeroacoustics. In addition, because customer comfort draws stricter acoustic regulation on electrical products, increasing interest about flow-induced noise generated from the products has led the development of a quiet cooling fan with same aerodynamic performance.

On the other hand, experimental methods about noise reduction and noise measurement have widely established in previous studies [1-3]. But expensive mock-ups and measurements derived by trial-and-errors cannot easily deal with a specific problem in the flow field related to flow noise generation. So, simulations by computational/numerical method, so called CFD/CAA have supported to understand and describe the unsteady and complex flow field in detail [4, 5]. The decrease of the turbulence by understanding the flow field with CFD/CAA has resulted in the noise reduction generated from fluid machinery like a fan. Not only comparison between experimental data and CFD/CAA results is used to validate and evaluate the predictive capability of the numerical method, but also CFD/CAA is used to provide additional information and explanation of the flow field and acoustic field which can derive the design modifications.

Basic methodology of CAA has established in 1990's, which the aerodynamic noise has been directly predicted using the base of the Lighthill's equation [4]. However, due to the difficulty for application of the equation, Jeon and Lee suggested an easier method using the Lowson's equation in the numerical calculation [5]. This method to calculate the noise term in CAA uses the static pressure fluctuation on all surface nodes of the fan in the unsteady state analysis from CFD results [6-8].

The present study is focused on the characteristics of the noise caused by the unsteady flow and the prediction for noise reduction on the axial fan. The three-dimensional Navier-Stokes equations were solved in this calculation through Large Eddy Simulation (LES) model to simulate the unsteady flow field. The aerodynamic noise analysis was calculated the using Ffowcs Williams and Hawkings (FW-H) equation.

2. Experimental apparatus

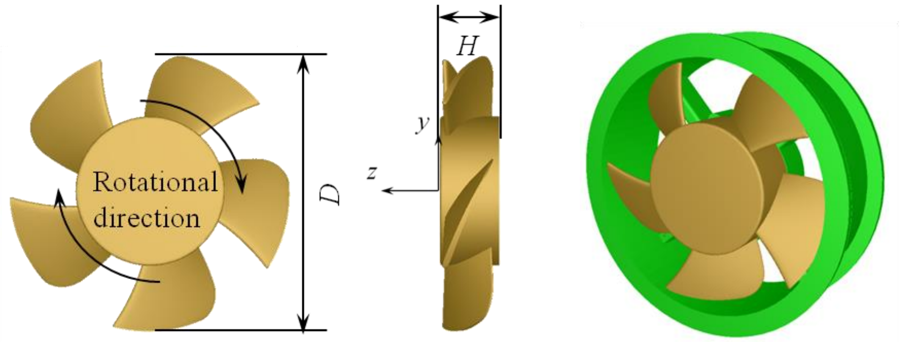

Figure 1: Tested fan shape

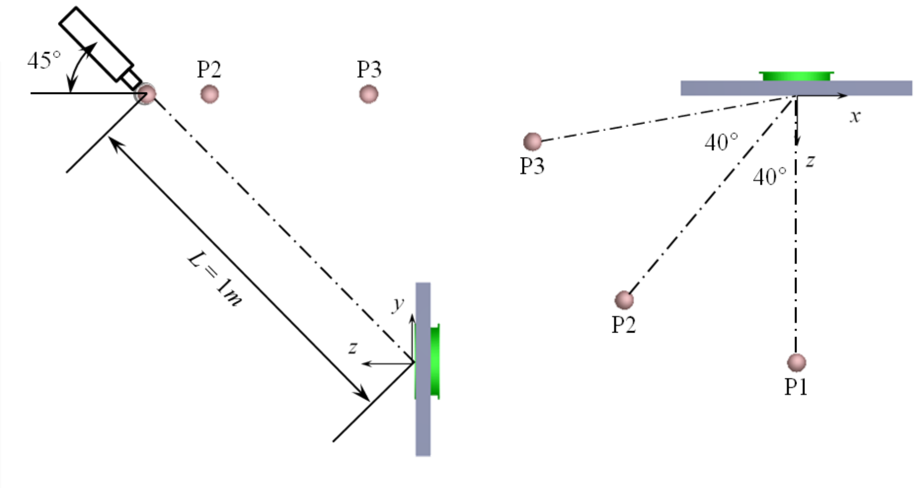

Figure 2: Microphone positions

The axial fan driven by AC motor was operated without the flow restriction to the external environment at N = 2850 rpm in a semi-anechoic room and also fixed by stringers for prevention of the structure-bone noise as shown Figure. 1. The diameter (*D*) and height (*H*) of the axial flow fan were 0.166 and 0.035 m, respectively. The microphone for measuring aerodynamic noise was installed with 45° at vertical direction at a distance 1 m far from the rotation axis of the fan as shown in Figure 2. The measurement was conducted at 3 points by changing the horizontal angle to 0°, 40° and 80°, respectively. The noise collected by the microphone was measured using a sound level meter, and the signal of the noise was analyzed with an FFT analyzer into frequency band components. In this case, the 1st BPF at 2850 rpm was observed at 237.5 Hz.

3. Numerical simulation

3.1 Numerical analysis of an unsteady flow field

In the study, a commercial code Cradle SCRYU/Tetra was used to calculate the three-dimensional flow field of the axial flow cooling fan. The Large Eddy Simulations (LES) was adopted since LES has practical advantage to aerodynamic noise prediction, compared with other unsteady calculation scheme such as URANS, DNS and so on.

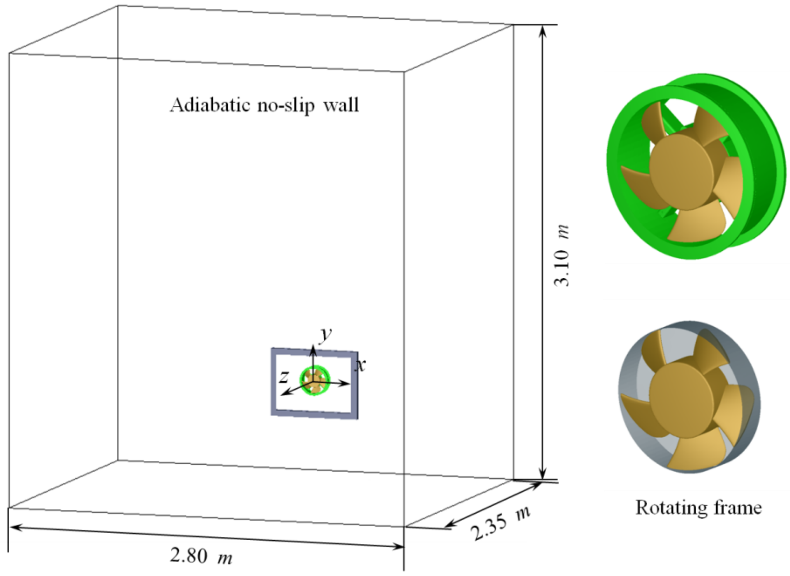

Figure 3: Computational domain and rotating frame at axial flow fan

Figure 3 shows the computational domain for numerical analysis and the shape of the axial flow fan in detail. The shape of computational domain was similar to that of the semi-anechoic room in which the noise was measured; the width, length, and height were 2.80 m × 2.35 m × 3.10 m, respectively. For the calculation region of the fan, the impeller was located in the rotating frame to simulate the rotation of the fan and the casing and semi-anechoic room except the impeller were set up in the stationary frame. Unstructured grids were used for the grid system including the two frames.

Figure 4 shows the computational grid system with five boundary layers in a direction perpendicular to the walls using prism element type, in order to satisfy $y^+ < 10$ at the 1st boundary layer and to predict correctly the velocity profile near the wall. For instance, the size of surface mesh on the impeller is 0.7 mm and the initial thickness of the prism perpendicular to the wall near a blade tip was 0.031 mm. The number of elements used in the grid system was approximately 16 million and the number of nodes was approximately 6.15 million.

In the boundary conditions, adiabatic no-slip conditions were used for the impeller, casing and the walls of the semi-anechoic room. The rotation speed of the impeller was 2850 rpm. The boundary surfaces between the rotating frame of reference and the stationary frame of reference were considered as surfaces of the sliding mesh. Also, the impeller and the inner surface of the casing which envelopes the impeller was named as the acoustic source area, in order to obtain the surface pressure fluctuation along the time for the aeroacoustic analysis.

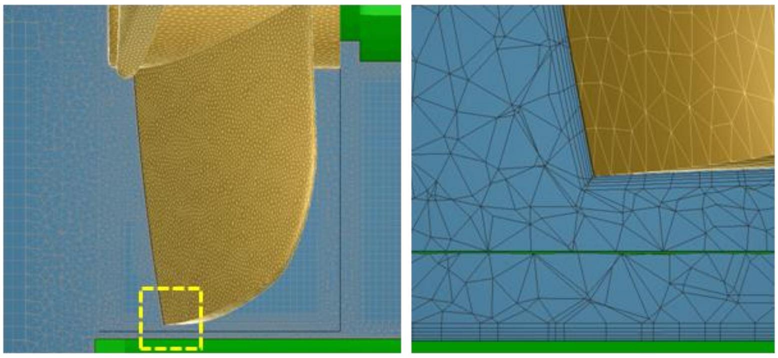

Figure 4: Computational grids

3.2 Prediction of aerodynamic noise from fan

According to previous study by Neise [11], it shows that dipole sound source is the dominant source in fan noise. In the present study, a numerical method for acoustic field analysis was applied to predict the acoustic sources generated by the rotating impeller and stationary casing. Eq.(1) can be derived from a basic fluid dynamics equation using generated functions, and it represents an in-homogeneous wave equation that follows the FW-H equation:

$$\left(\frac{1}{a_0^2}\frac{\partial^2}{\partial t^2}-\frac{\partial^2}{\partial x_i^2}\right)p' = \frac{\partial}{\partial t}\left[\rho v_n \delta(f)\nabla f\right]-\frac{\partial}{\partial x_i}\left[n_i \rho \delta(f)\nabla f\right]+\frac{\partial}{\partial x_i}\left[T_{ij}H(f)\right]. \tag{1}$$

where,	p'	:	Sound pressure [Pa]
	ρ	:	Air density [kg/m^3]
	n_i	:	Surface normal
	a_0	:	Speed of sound [m/s]
	v_n	:	Normal surface velocity [m/s]
	p	:	Static pressure [Pa]
	T_{ij}	:	$\rho u_i u_j + p_{ij} - a_0^2 \rho \delta_{ij}$ Lighthill stress tensor [Pa]
	$\delta(f)$	:	Dirac-delta distribution
	$H(f)$	:	Heaviside function

The first, second, and third terms on the right side of Eq.(1) represent the monopole, dipole and quadrupole, respectively. In the present study, only the dipole term in Eq.(1) was considered and the relevant force was expressed as a point force. Then, Eq. (1) can be organized as shown in Eq. (2):

$$p'_d = \frac{1}{4\pi c_0}\int_s \left[\frac{r_i}{r^2(1-M_r)^2}\times\left(\frac{\partial}{\partial \tau}\left\{n_i \cdot p_{fluid}(y_i,\tau)\right\}+\frac{n_i \cdot p_{fluid}(y_i,\tau)}{1-M_r}\frac{\partial M_r}{\partial \tau}\right)\right]d\sigma . \tag{2}$$

This equation indicates that the aeroacoustic pressure for a moving point force can be calculated using the time variation of force and acceleration. c_0 is the speed of sound, p_{fluid} is the surface pressure by fluid from flow analysis, and r is the distance between the observer and the noise source. x and y represent the locations of the observer and the noise source, respectively. M_r is the moving speed of the sound source defined as follows:

$$M_r = \frac{(x_i - y_i)}{r}M_i . \tag{3}$$

By applying Eq. (2) to each grid point of the blade and the inner surface of the casing, which comprise the acoustic source area used for the CFD analysis, acoustic pressure in the free field can be predicted. In this study, the effects of scattering, reflection, and refraction by the casing in the acoustic field were not considered, and the calculation was conducted only for the characteristics of the noise source and its radiation in the free field.

The part within the square bracket in Eq. (2) can be defined as aeroacoustic source strength:

$$\text{Aeroacoustic source strength} = \frac{r_i}{r^2} \times \left(\frac{\partial}{\partial \tau} \{ n_i \cdot p_{fluid}(y_i, \tau) \} + \frac{n_i \cdot p_{fluid}(y_i, \tau)}{1 - M_r} \frac{\partial M_r}{\partial \tau} \right). \quad (4)$$

This equation indicates that the pressure fluctuation by fluid is related with the acoustic source strength. As shown in Eq. (4), it is known that this acoustic source is radiated in the acoustic pressure terms.

4. Results and discussion

4.1 Unsteady flow field and noise source

As noted before, the pressure fluctuation on the solid surface in the unsteady flow field is needed for the analysis of the aerodynamic noise. First, the result of steady-state calculation was obtained as an input condition for unsteady flow analysis. The characteristics of static pressure fluctuation by the unsteady flow field for the discussion were considered after two rotations of the impeller. The first unsteady state analysis was conducted continuously by up to eight rotations with the time step by 29.2 μs per iteration. Then, the second unsteady state analysis was conducted by five rotations, in order to develop unsteadiness in the flow field completely. In the second step, the time step per iteration was changed to 25.7 μs because the sampling data for accurate FFT analysis needs the number of 2 to the power of n. Each sub-iteration was also performed for obtaining the solution accurately. In addition, the residual for each velocity component and pressure was set to 1.0E-6 and 1.0E-5 as the convergence condition about each iteration.

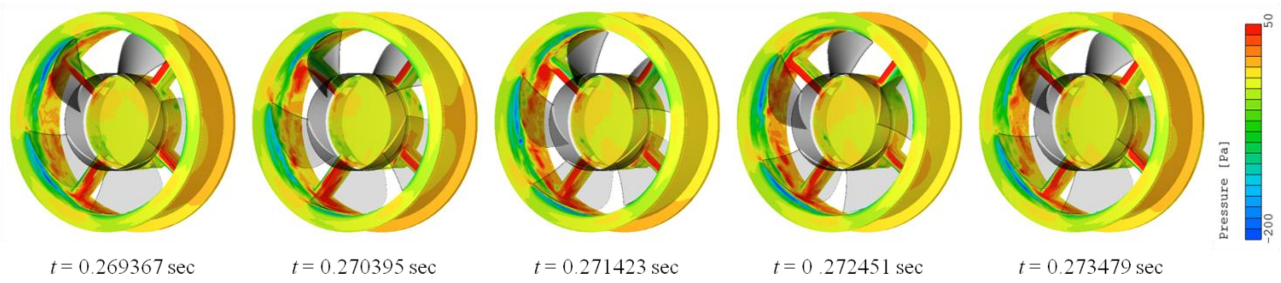

Figure 5: Static wall pressure distribution on casing depending on impeller rotation

Figure 5 shows the distribution of static pressure on the inner surface of the casing. As the impeller rotates, the static pressure distribution on each strut and the inner surface of casing changed continuously. Especially, as the blade was getting closer to each strut, the static pressure on the inner surface near the blade tip was decreased suddenly. It indicates that the pressure fluctuation as the BPF noise source was caused by not only the pressure potential along the blade but also the stronger tip vortex. The static pressure distribution near the root of the strut was changed continuously by the interaction between the spiral flow by the impeller and the strut. This phenomenon was expected to be BPF noise source because an abrupt change of the surface pressure was synchronized with the impeller rotation.

Figure 6 shows the vorticity on the *yz* plane at $x = 0$. The vortices detached from the edge of the casing have been generated continuously due to fan rotation. The interaction between a detached vortex and a blade has generated the strong vorticity at the downstream which the tip of the leading edge passed through. The strong vortices destroyed by the next blade caused to the fluctuation of static pressure on the blade. It seemed that the random fluctuation of the tip vortex is one of turbulent noise source.

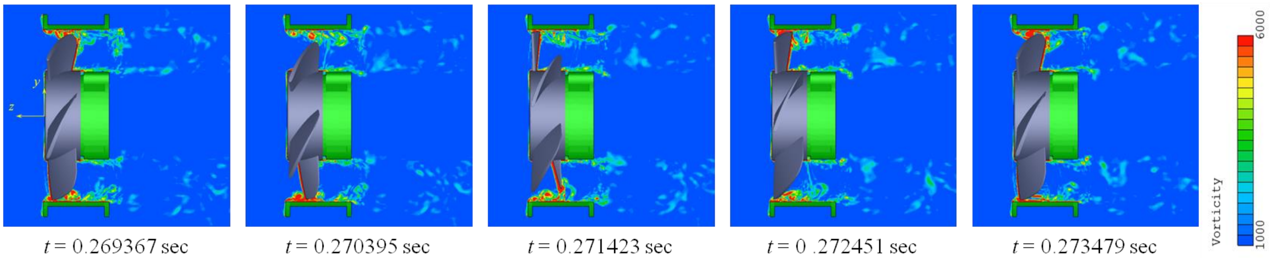

Figure 6: Vorticity distribution on the *yz* plane at *x* = 0 depending on impeller rotation

4.2 Aerodynamic noise prediction and modification

Figure 7 shows the comparison of the noise spectra obtained by the numerical analysis and the experimental measurement. The emitted sound pressure was calculated using the Ffowcs Williams and Hawkings equation. The sound spectrum and tonal/broadband noise predicted by the numerical analysis up to 1200 Hz was similar to those of the noise measured by the experiment but the noise prediction discrepancy appeared at higher frequency over 1kHz.

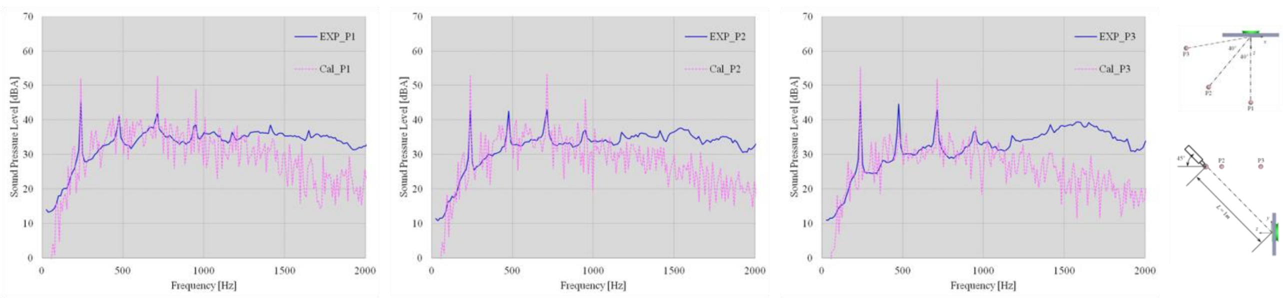

Figure 7: Comparison of noise spectra obtained by calculation and experiment

Figure 8 shows the calculated aeroacoustic source strength of the axial flow fan. It was found that the dominant noise sources on the impeller were located at the leading edge tip of the blades and the blade surface on pressure side and the dominant noise sources on the casing were distributed near the area where the leading edge tip of blades passed through.

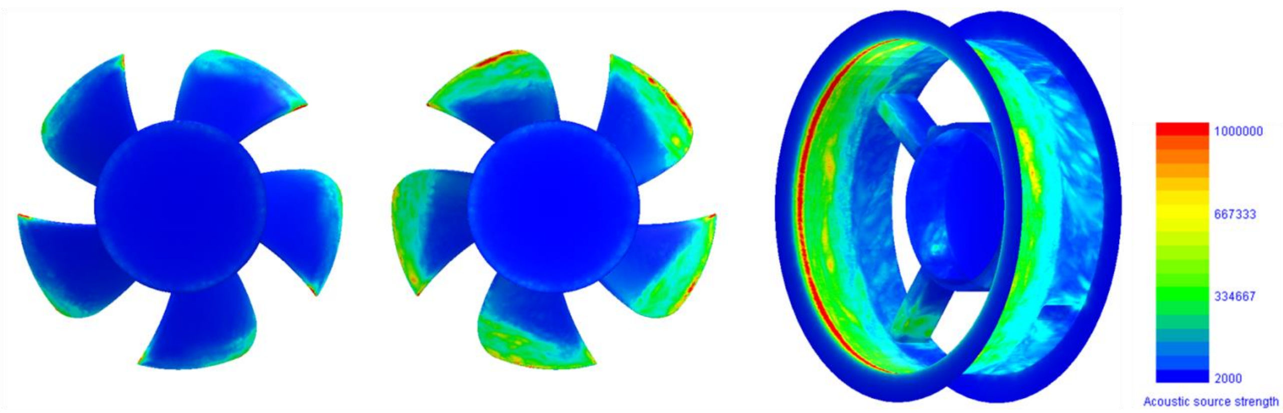

Figure 8: Distribution of aeroacoustic source strength on impeller and original casing

In order to examine the effect of the shape modification on the noise reduction, the inlet curvature of the casing was changed and compared in the simulation. Figure 9 shows the comparison of the noise spectra for the original and modified casing and the vorticity distribution on the modified casing. In the vorticity distribution, detached vortices from the edge of casing were removed at the flow field. In the simulation, the modified casing has resulted in noise reduction which OASPL was lower than that of the original casing by 1dB.

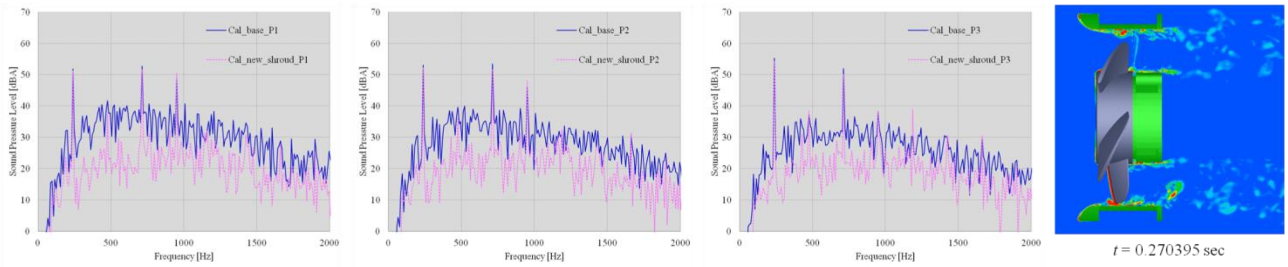

Figure 9: Comparison of noise spectra for original and modified casing

and vorticity distribution on modified casing

Figure 10 shows the aeroacoustic source strength of the axial flow fan with modified casing. The strength of the sound sources was reduced entirely. In particular, the sound sources on the pressure side of the impeller were reduced substantially. So, it is effective for noise reduction to perform the simulation with modified shape and compare result with original one.

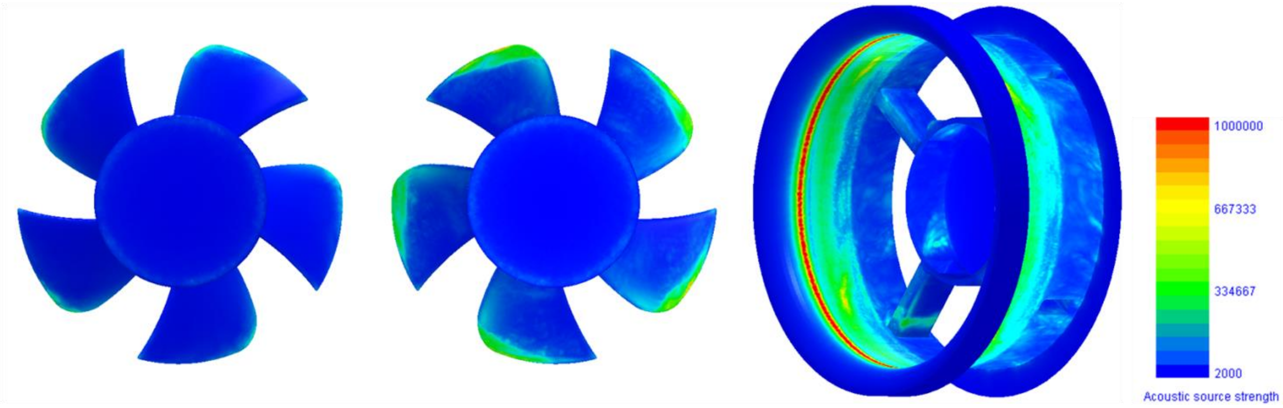

Figure 10: Distribution of aeroacoustic source strength on impeller and modified casing

5. Conclusions

In this study, the characteristics for aerodynamic noise and the noise reduction of a small axial flow cooling fan were predicted using three-dimensional flow analysis and the Ffowcs Williams and Hawkings equation. The results of this study are as follows.

(1) The unsteady flow analysis in the base model showed that strong vortexes at the behind of each blade was generated through the clearance of the blade and the casing, the interaction between detached vortexes from the edge of casing and the blades. It was expected that the vortexes destroyed by the next blade affected the static pressure fluctuation on the blade of pressure side. From the acoustic source strength, it was found that the blade of pressure side, the blade leading edge tip and the casing's inner area close to the blade leading edge tip are the dominant aeroacoustic sources, respectively.

(2) The modified casing with a curvature at the front was applied to the purpose for noise reduction. The modified casing which removes the complex flow from the edge made the inlet flow field uniform. The region of sound sources on pressure side of the impeller was reduced dramatically by the elimination of detached vortexes from the edge of the casing. It has resulted in at least OASPL 1 dB noise reduction.

REFERENCES

1 Cattanei, A., Ghio, R., Bongiovì, A. Reduction of the tonal noise annoyance of axial flow fans by means of optimal blade spacing, *Applied Acoustics*, **68** (11-12), 1323-1345, (2007).

2 Ito, T., Minorikawa, G. and Fan, Q. Experimental research for performance and noise of small axial fan, *International Journal of Fluid Machinery and Systems*, 2 (2), 136-146, (2009).

3 Neise, W. Noise reduction in centrifugal fans: A literature survey, *Journal of Sound and Vibration*, **45** (3), 375-403, (2010).

4 Lee, S. Kim, H. J. and Runchal, A. Large eddy simulation of unsteady flows in turbomachinery, *Proceedings of the Institution of Mechanical Engineers, Part A: Journal of Power and Energy*, 218 (7), 463-475, (2004).

5 Fontanesi, S., Paltrinieri, S. and Cantore, G. CFD analysis of the acoustic behaviour of a centrifugal compressor for high performance engine application, *Energy Procedia*, 45, 759-768, (2014).

6 Lighthill, M. J. On sound generated aerodynamically, I. General Theory, *Proc. Roy. Soc.*, A211, 564-587, (1952).

7 Jeon, W. H. and Lee, D. J., An analysis of the flow and aerodynamic acoustic sources of a centrifugal impeller, *Journal of Sound and Vibration*, **222** (3), 505-511, (1999).

8 Lim, T. G., Jeon, W. H. and Minorikawa, G. Characteristics of unsteady flow field and flow-induced noise for an axial cooling fan used in a rack mount server computer, *Journal of Mechanical Science and Technology*, **30** (10), 4601-4607, (2016)

9 Jeon, W. H., Baek, S. J. and Kim, C. J. Analysis of the aeroacoustic characteristics of the centrifugal fan in a vacuum cleaner, *Journal of Sound and Vibration*, **268** (5), 1025-1035, (2003).

10 Kim, W., Jeon, W. H., Hur, N., Hyun, J. J., Lim, C. K. and Lee, S. H. Development of a low-noise cooling fan for an alternator using numerical and DOE methods, *International Journal of Automotive Technology*, **12** (2), 307-314, (2011).

11 Neise, W. Review of fan noise generation mechanism and control methods, *Proceedings of International INCE Symposium of Fan Noise*, France, 45-56, (1992).